Video Article

Four-color Fluorescence Immunohistochemistry of T-cell Subpopulations in Archival Formalin-fixed, Paraffin-embedded Human Oropharyngeal Squamous Cell Carcinoma Samples

Simone Punt[1], Robert J. Baatenburg de Jong[2], Ekaterina S. Jordanova[1,3]

[1]Department of Pathology, Leiden University Medical Center

[2]Department of Otorhinolaryngology and Head and Neck Surgery, Erasmus University Medical Center

[3]Center for Gynecological Oncology Amsterdam, VU Medical Center

Correspondence to: Simone Punt at S.vd.Garde@outlook.com

URL: https://www.jove.com/video/55589
DOI: doi:10.3791/55589

Keywords: Cancer Research, Issue 125, Immunology, head and neck cancer, tumor microenvironment, fluorescence microscopy, T cell, Th17 cell, Treg, IL-17

Date Published: 7/29/2017

Citation: Punt, S., Baatenburg de Jong, R.J., Jordanova, E.S. Four-color Fluorescence Immunohistochemistry of T-cell Subpopulations in Archival Formalin-fixed, Paraffin-embedded Human Oropharyngeal Squamous Cell Carcinoma Samples. *J. Vis. Exp.* (125), e55589, doi:10.3791/55589 (2017).

Abstract

The four-color fluorescence immunohistochemistry (IHC) technique is a method to quantify cell populations of interest while taking into account their relative distribution and their localization in the tissue. This technique has been extensively applied to study the immune infiltrate in various tumor types. The tumor microenvironment is infiltrated by immune cells that are attracted to the tumor site. Different immune cell populations have been found to play different roles in the tumor microenvironment and to have a different impact on the outcome of disease. This manuscript describes the use of multiparameter fluorescence IHC on oropharyngeal squamous cell carcinoma (OPSCC) as an example. This technique can be extended to other tissue samples and cell types of interest. In the presented study, we analyzed the intraepithelial and stromal compartment of a large OPSCC cohort (n = 162). We focused on total T lymphocytes ($CD3^+$), immunosuppressive regulatory T cells (Tregs; *i.e.,* $FoxP3^+$), and T helper 17 (Th17) cells (*i.e.,* $IL\text{-}17^+CD3^+$) using a nuclear counterstain to distinguish tumor epithelium from stroma. A high number of T cells was found to be correlated with improved disease-free survival in patients with a low number of intratumoral $IL\text{-}17^+$ non-T cells. This suggests that $IL\text{-}17^+$ non-T cells may be correlated with a poor immune response in OPSCC, which is in agreement with the correlation described between IL-17 and poor survival in cancer patients. Currently, novel multiparameter fluorescence IHC techniques are being developed using up to 7 different fluorochromes and will enable the more precise characterization and localization of immune cells in the tumor microenvironment.

Video Link

The video component of this article can be found at https://www.jove.com/video/55589/

Introduction

Oropharyngeal squamous cell carcinomas (OPSCCs) are a heterogeneous group of squamous cell cancers originating in the oropharynx. Risk factors for OPSCC include human papillomavirus (HPV) infection and alcohol and tobacco use[1,2]. The role of the immune response and how to use this in a clinical setting is just starting to be explored. The tumor microenvironment is infiltrated by immune cells that are attracted to the cancer site. Although a high $CD8^+$ cytotoxic T-cell frequency has been correlated with improved survival in OPSCC patients[3], the role of other T-cell subsets, including Tregs and Th17 cells, is still unclear[4]. Whereas Th1 and Th17 cells are supposed to aid in the immune response targeting tumor cells, Tregs are well known for their abilities to suppress the activity of other T cells[5]. However, the presence of Tregs has been found to correlate with both favorable and unfavorable responses in different tumor types[6]. Since not all immune cells present in the blood infiltrate the tumor to the same extent, studying the local tumor microenvironment provides the most reliable measure of the immune response directed against the tumor. The aim of this study is to determine the correlation between the numbers and types of immune cells and the clinical outcome. We used four-color fluorescence IHC imaging to analyze the number and localization of various T-cell subpopulations in human OPSCC.

We focused on total T lymphocytes ($CD3^+$), Th17 cells, and immunosuppressive $FoxP3^+$ Tregs, whose differentiation pathway is closely related to Th17 cells. Th17 cells are characterized by the combination of CD3 and IL-17. The cytokine IL-17 can also be produced by non-T cells[7]. We determined the distribution of intra-epithelial and stromal T cells, Tregs, Th17, and $IL\text{-}17^+$ non-T cells in a large series of OPSCC cases and analyzed the correlations with patient survival. Multicolor fluorescence IHC was used to identify the expression of CD3, Foxp3, and IL-17, in combination with a DAPI counterstain. This assay allowed for the easy and clear identification of both tumor cells (using DAPI nuclear staining) and the infiltrating T-cell populations (using a combination of different markers). Following sample preparation and staining, a fluorescent microscope and imaging software were used to separate the different fluorescent colors used and to determine the number and type of cells present in both the tumor epithelium and the tumor-associated stroma.

Copyright © 2017 Journal of Visualized Experiments

An alternative assay to quantify and phenotype immune cell populations is flow cytometry analysis, or cytometry by time of flight (CyTOF) analysis, of tumor or peripheral samples (*i.e.,* blood or ascites). Using this technique, all information about localization and relative distribution of the different cell types is lost. The use and analysis of peripheral samples also does not provide information about which cells are able to infiltrate the tumor microenvironment. Blood and ascite immune-cell analyses have been shown not to reflect the phenotype and frequency of immune cell infiltration of the tumor tissue[8,9].

Another alternative is the use of bright-field microscopy. An advantage of this technique over fluorescence imaging is the absence of tissue autofluorescence. Although some samples contain more autofluorescence—particularly erythrocytes, but also other cell types, including neutrophilic granulocytes—these areas can easily be removed in the analysis of almost all samples. Immunofluorescence offers the advantage of analyzing multiple markers in one sample by using a panel of targeted fluorescent wavelengths. This is currently impossible to the same extent for bright-field microscopy due to the lack of a sufficient number of labels and commercially available antibody isotypes for a particular antigen.

The multicolor fluorescence IHC technique described here has been used in many different cancer types and antibody combinations to study different immune cell populations, as well as tumor cell-expressed molecules, such as human leukocyte antigens (HLA) and PD-L1[10,11,12]. The protocol has been established and validated using many different types of samples and antibodies.

Protocol

Patient samples were handled according to the medical ethical guidelines described in the Code of Conduct for Proper Secondary Use of Human Tissue of the Dutch Federation of Biomedical Scientific Societies (www.federa.org).

1. Prepare Slides

1. Obtain resected tissue material (any kind of tissue) from a pathology department after obtaining medical ethical committee permission to use resected material.
   NOTE: For the current experiment, pretreatment tumor samples were obtained from primary oropharyngeal tumors diagnosed in the Leiden University Medical Center, Leiden, the Netherlands between 1970 and 2011, selected as described before (n = 162)[13]. The size of the tissue was only limited by the requirement for a sufficient amount of tumor tissue to reliably take 4 microscopic images inside the tumor.
2. Fix the tissue in 4% buffered formalin for a minimum of 12 h. Dehydrate the tissue in a graded series of ethanol. Wash it in xylene and embed it in paraffin wax using an automated tissue processor.
3. **Cut 4 µm-thick formalin-fixed, paraffin-embedded (FFPE) tissue sections on glass slides using a microtome. Place the tissue block in the microtone tissue holder using standard procedures.**
   1. Cut ribbons of tissue and lay them on the surface of a water bath containing deionized water at 45 ºC. Use a slide suitable for immunohistochemical staining to fish out a section by placing the slide in the water directly underneath the section. Carefully move the slide up at an angle, taking the section out of the water and sticking it onto the slide.
4. Let the slides dry overnight at 37 °C.
5. Deparaffinize the FFPE slides by immersing them completely in fresh 100% xylene, three times for 5 min each. Rehydrate the slides by submerging them twice in fresh 100% ethanol, 70% ethanol, and 50% ethanol for 5 min each.

2. Perform Antigen Retrieval

1. Wash the slides in deionized water for 5 min.
2. Preheat Tris-ethylenediaminetetraacetic acid (EDTA) buffer (10 mM Tris plus 1 mM EDTA, pH 9.0) to boiling temperature using a microwave. Perform antigen retrieval by submerging the slides in the preheated EDTA buffer and keeping the buffer at this temperature for 10 min in the microwave.
   NOTE: Any microwave with a power of 900 W can be used.
3. Let the slides cool down in the buffer for 2 h.

3. Stain Tissue Slides

1. Wash the slides twice with phosphate-buffered saline (PBS) for 5 min each.
2. Draw a circle around the tissue with a hydrophobic pen to prevent the diluted antibodies from spilling off the slide. Wash once more with PBS; this is optional.
3. Incubate the tissue with primary antibodies (anti-CD3 1:50, anti-FoxP3 1:200, and anti-IL-17 1:50) diluted in 1% w/v bovine serum albumin (BSA) in PBS at room temperature overnight.
   NOTE: The volume per slide depends on the size of the tissue, but it is typically 50 - 150 µL. Substitute the primary antibodies with antibodies of the same isotype class with an unknown specificity for the negative control slides at the same dilution as the CD3, CD8, and FoxP3 antibodies (*i.e.,* rabbit Ig isotype control antibody, mouse IgG1 isotype control antibody, and goat IgG isotype control antibody).
4. Wash the slides three times with PBS for 5 min each.
5. **Incubate the tissue with a combination of fluorescently labeled secondary antibodies targeting the primary antibody species and/or isotypes (*i.e.,* 1:200 donkey anti-goat IgG Alexa 488, donkey anti-rabbit IgG A546, and donkey anti-mouse A647) diluted in 1% BSA in PBS at room temperature for 1 h.**
   NOTE: The volume per slide depends upon the size of the tissue but is typically 50 - 150 µL.
   1. After adding the secondary antibody, keep the slides protected from light as much as possible by storing them in a dark box or by wrapping the box in aluminum foil.

4. Mount and Counterstain Tissue Slides

1. Wash the slides three times in PBS for 5 min each.
2. Mount the slides using an aqueous anti-fade mounting medium containing a nuclear counterstain (*e.g.,* DAPI). Analyze the slides using a fluorescent microscope as soon as possible (within two weeks). Store the slides in the dark at 4 °C until analysis.

5. Analyze Stained Tissue Slides

1. **Obtain four images of each slide using a fluorescence microscope equipped with a 20 - 25X objective. Take images at random locations throughout the total tumor area included in the slide to capture a representative fraction of the tumor.**
   NOTE: A standard magnification of 250X should be used. Any fluorescent or laser scanning microscope can be used, provided it has the filters and lasers needed to visualize the fluorochromes used.
   1. For visualization of Alexa 488, use an excitation maximum of 490 and an emission maximum of 525; for visualization of Alexa 546, use an excitation maximum of 556 and an emission maximum of 573; for visualization of Alexa 647, use an excitation maximum of 650 and an emission maximum of 665; and for visualization of DAPI, use an excitation maximum of 358 and an emission maximum of 461.
   2. Save the images as image files (*i.e.,* jpeg and tiff) in the software available to the user.

2. **Discriminate between tumor epithelium and tumor stroma areas based on the nuclear and cellular shapes of tumor epithelial versus stromal cells after consulting a pathologist.**
   1. To determine the total stromal surface area, draw a line around all area(s) occupied by stromal cells (rather than tumor cells) and record the surface area using the image analysis software provided by the microscope manufacturer.
      1. Click on the "Overlay" tab under the image; choose the "Closed Poly-line" shape and click on it. Demarcate the boundary between tumor epithelial and stromal fields by clicking around the area until reaching the first point again.; this provides a measure for that area.
         NOTE: Once the shape is closed, a number will appear next to the shape encircling the surface area of the selected image (A = x μm^2).
   2. Subtract this surface area from the total image surface area (provided in image properties) to calculate the epithelial surface area. Exclude vascular, necrotic, and autofluorescent areas by drawing a line around them, recording the size of the provided area and subtracting that from the epithelial surface area.
   3. Save all surface area numbers in a spreadsheet file to calculate the average surface areas and cell numbers per slide.
   4. Using the image analysis software, determine if the cells are single-, double-, or triple-positive by checking the fluorescence of all four channels.
      1. Count the single-, double-, and triple-positive cells in each image using ImageJ.
         1. Download ImageJ. Open an image by clicking on "File" and "Open" and selecting the image to be analyzed. Right-click on the "Point Tool" (a red square in the middle of four lines) and select the "Multi-Point Tool." Double-click on the "Multi-Point Tool" and count the number of different cell types in the image by selecting a different counter number for each cell type.
            NOTE: Count all the cells of each different cell type, as identified by the presence of one, two, or all three fluorescent colors. Exclude DAPI, as this nuclear counterstain is present in all cells and is used to discriminate tumor cells from immune cells. Each cell type is counted using a different counter number. Count the cell numbers of each cell type separately in the tumor epithelial and stromal areas by choosing a different counter number each time. Do not count cells within blood vessels and largely autofluorescent areas.
         2. Record the number of cells analyzed in each counter bin for each image in a spreadsheet file.
         3. Divide the total number of cells for each cell type over the total surface area of tumor epithelium and tumor stroma analyzed.

6. Statistical Analysis

NOTE: All statistical analyses should be discussed with a statistician to assure quality of data. For general statistics, use any medical statistics guide[14].

1. Test the correlations between cell frequencies using a Spearman's rank correlation rho test.
2. Test the statistical differences in the numbers of positive cells between patient groups using the Wilcoxon Mann-Whitney test.
3. Test the correlations between cell numbers and disease-free survival (*i.e.,* time from diagnosis until local or distant recurrence of death or disease) by dividing the patients in groups based on a cut-off number of cells using Kaplan-Meier curve generation and log rank analysis[15].
4. Perform multivariate analyses using Cox proportional hazard regression analysis.

Copyright © 2017 Journal of Visualized Experiments

Representative Results

A series of FFPE pretreatment tumor samples obtained from primary oropharyngeal tumors diagnosed in the Leiden University Medical Center, Leiden, the Netherlands between 1970 and 2011, selected as described before (n = 162), was stained using the protocol described[13]. One to four random images of each slide were analyzed (**Figure 1**). Some autofluorescent cells are indicated, which can clearly be distinguished by their complete yellow appearance. Cells truly double- or triple-positive only stain positive for a particular antibody at the expected localization, which is at the cell membrane or the nucleus, in this case. Negative control slides did not show any specific staining above background tissue autofluorescence (**Figure 2** and **Figure 4**), confirming that all signal is specific to the targets recognized by the primary antibodies. All tumor samples were found to be infiltrated by $CD3^+$ T cells to varying extents. $FoxP3^+$ Tregs always expressed CD3 and were one of the major infiltrating T-cell populations. CD3 cells expressing IL-17 (Th17 cells) were a minor population of the infiltrating T cells. IL-17 expressed by $CD3^-$ cells was another abundant infiltrating cell population. $IL\text{-}17^+$ $FoxP3^+$ cells comprised no more than 0.01% of all $FoxP3^+$ cells.

All statistical tests were two-sided, and p-values below 0.05 were considered significant[14]. The correlations between intra-epithelial or total cell numbers and survival are presented, since the correlations between stromal or total cell numbers and patient survival were similar. A high number of infiltrating total $CD3^+$ T cells showed a trend toward a correlation with improved disease-free survival (0.086, **Figure 5A**) as compared to a low number of T cells (*i.e.,* lowest quartile). When specifically studying patients with a low number of $IL\text{-}17^+$ cells, a high number of total infiltrating T cells was correlated with improved disease-free survival (p = 0.012, **Figure 5B**). The prognostic effect of tumor-infiltrating T cells was lost in the group of patients with a high number of tumor-infiltrating $IL\text{-}17^+$ cells (data not shown). Thus, the effect of tumor-infiltrating T cells in OPSCC may be related to the low number of $IL\text{-}17^+$ cells present.

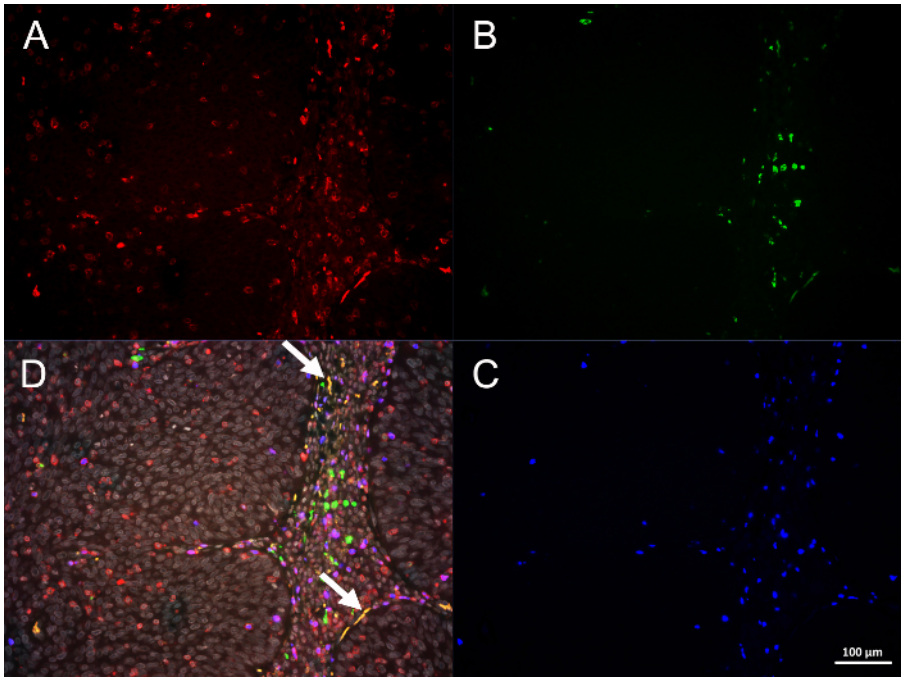

Figure 1: FFPE Oropharyngeal Cancer Tissue Stained by Four-color Fluorescence IHC. Representative image of an immunofluorescent stain for CD3 (**A**, red), IL-17 (**B**, green), and FoxP3 (**C**, blue), as well as the merged image combined with DAPI (gray) (**D**). Two autofluorescent cells are indicated by the arrows. Please click here to view a larger version of this figure.

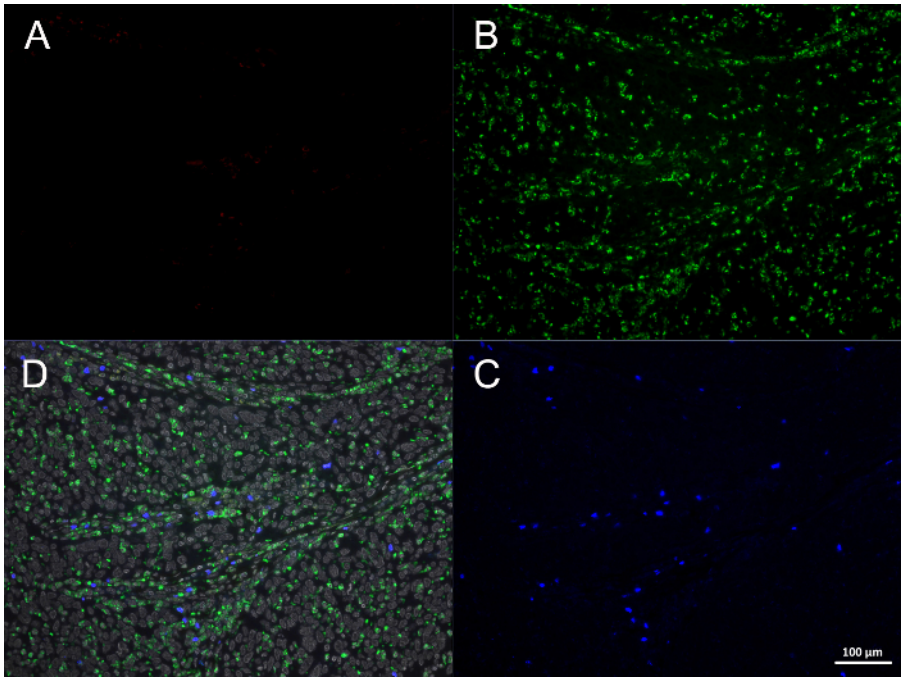

Figure 2: Negative Control for CD3. Representative image of FFPE oropharyngeal cancer tissue, stained as described in the protocol, substituting the anti-CD3 antibody with a rabbit Ig isotype control antibody with unknown specificity. No staining for rabbit Ig (**A**, red) combined with staining for IL-17 (**B**, green), FoxP3 (**C**, blue), and DAPI (**D**, gray) is shown. Please click here to view a larger version of this figure.

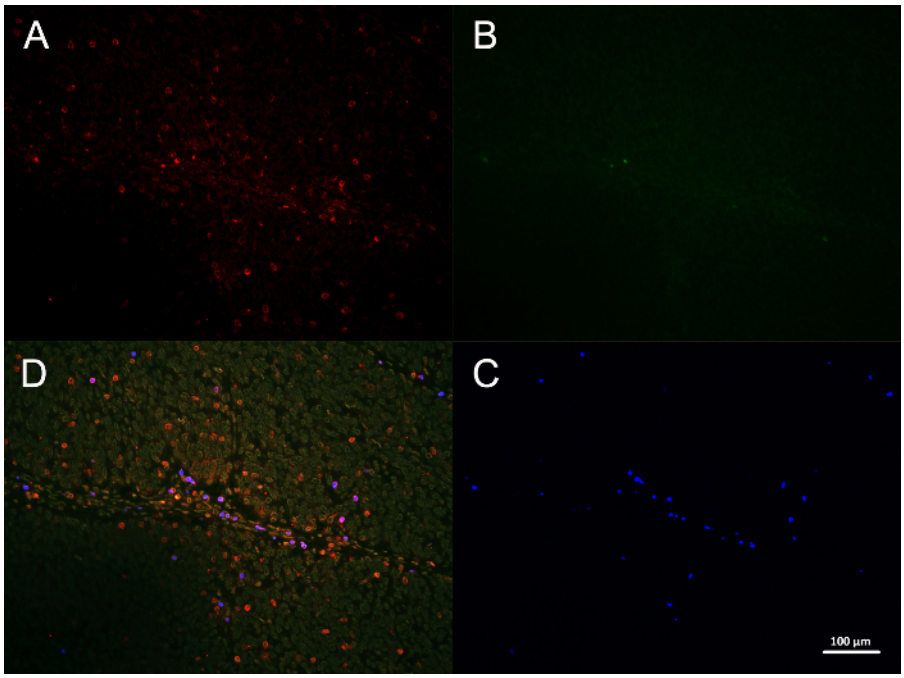

Figure 3: Negative Control for IL-17. Representative image of FFPE oropharyngeal cancer tissue, stained as described in the protocol, substituting the anti-IL-17 antibody with a goat Ig isotype control antibody with unknown specificity. No staining for goat Ig (**B**, green) combined with staining for CD3 (**A**, red), FoxP3 (**C**, blue), and DAPI (**D**, gray) is shown. Please click here to view a larger version of this figure.

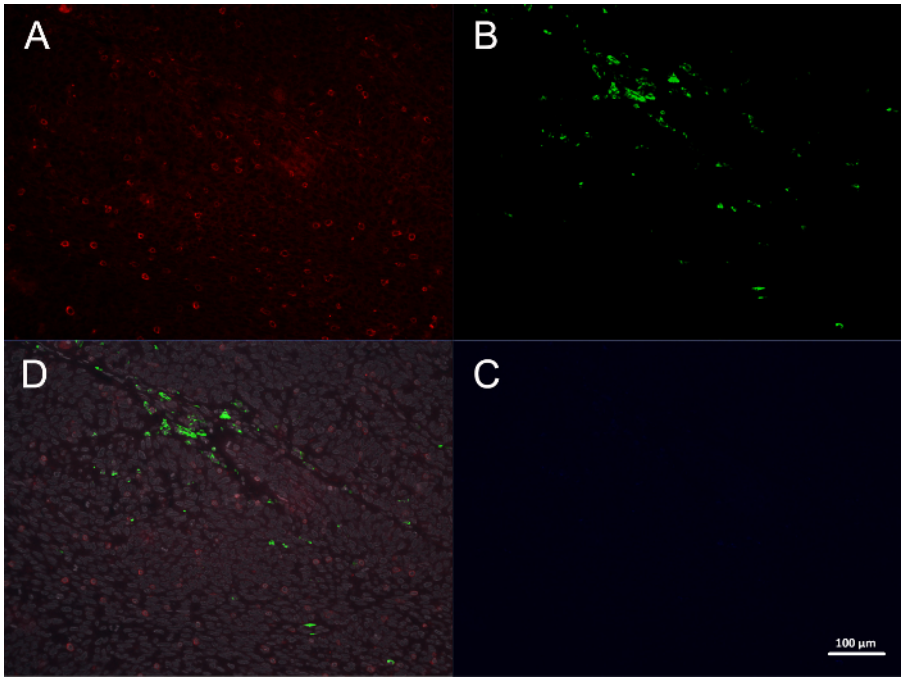

Figure 4: Negative Control for FoxP3. Representative image of FFPE oropharyngeal cancer tissue, stained as described in the protocol, substituting the anti-FoxP3 antibody with a mouse IgG1 isotype control antibody with unknown specificity. No staining for mouse IgG1 (**C**, blue) combined with staining for CD3 (**A**, red), IL-17 (**B**, green), and DAPI (**D**, gray) is shown. Please click here to view a larger version of this figure.

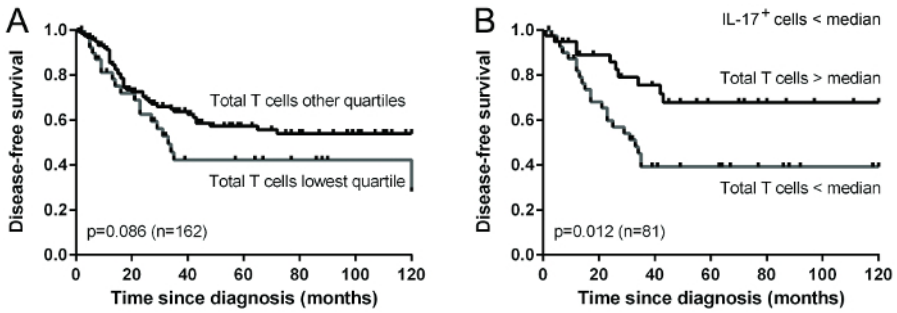

Figure 5: Kaplan-Meier Survival Curves. For patients with a below-median number of IL-17$^+$ cells/mm^2, disease-free survival curves are shown for a very low (*i.e.,* lowest quartile) versus high number of total T cells (**A**) and a low (*i.e.,* below median) versus high number of total T cells (**B**) in the total tumor area. Reproduced with permission from the Cancer Immunology Immunotherapy journal[13]. Please click here to view a larger version of this figure.

Discussion

For the protocol described, one of the most critical steps is to determine the correct dilution of the primary antibodies used. The dilution of the labeled secondary antibodies was 1:200, as recommended by the manufacturer of these specific Alexa-labeled antibodies. The dilution of the primary antibodies should then be determined by a serial dilution, preferably using two different samples of the intended tissue type (in this case, OPSCC). The optimal working dilution is the dilution at which a clear signal is obtained, without background noise and in the absence of a signal for the negative control at the same concentration. Modifications can be made with regard to the type of secondary antibodies and mounting medium used, depending on the type of microscope available and the preference of the researcher. If the intended results are not achieved, we recommend looking into the type of glass slides used, as some are known to cause problems with background signals for particular kinds of staining solutions (*e.g.,* Perma Blue). Second, some antigens may be disrupted by the use of heat-induced epitope retrieval. In that case, the researcher can replace the heating step of the buffer with other techniques, such as enzyme-induced epitope retrieval. Third, if using the hydrophobic pen, the marking should not be made too close to the tissue, as this will prevent the staining solution from working properly. Regarding the number of sections per sample and the required number of images per section, it is up to the researcher and the specific research question to determine the number required to answer the research question with sufficient statistical power. For our analysis, we used one section per sample and four images per section. Finally, when using immunofluorescent staining, care should be taken when using nail polish to seal the cover slips, as alcohol present in the nail polish solution can affect the fluorescent signal.

The protocol described here does not involve high-throughput analysis. We have tried to automate this step, but the subjective interpretation of cellular size and morphology complicates the automation of the analysis with the software packages available at the time. Although tissue preparation and staining can be automated to a great extent, the counting of the cells was performed manually.

Copyright © 2017 Journal of Visualized Experiments

We were able to study the correlations between the infiltrating T-cell subsets studied and clinical outcome using the described protocol. A high number of T cells was found to be correlated with improved disease-free survival in patients with a low number of intratumoral IL-17$^+$ non-T cells. This suggests that IL-17$^+$ non-T cells may be related to a poor immune response in OPSCC, which is in agreement with the correlation described between IL-17 and poor survival in cancer patients[16].

Improved software programs have now become commercially available to automate this step and are currently replacing the manual cell observation and counting, which will lead to more reliable, objective, reproducible, and fast results.

In addition, the availability of commercial kits allowing for the multiplexing of fluorescent immunohistochemical markers is currently on the rise[17]. This will allow for the multiplexing of up to 7 different immune markers/biomarkers in combination with a nuclear counterstain. However, we believe that the protocol reported here will still be more efficiently and easily applied in laboratories lacking complex and expensive infrastructure, microscopes, and software packages for multispectral staining analysis.

Disclosures

The authors declare no commercial or financial conflict of interest.

Acknowledgements

Simone Punt was supported by grant UL2010-4801 from the Dutch Cancer Society. We would like to thank all the co-authors of the original paper that this JoVE protocol is based on: Emilie A. Dronkers, Marij J. P. Welters, Renske Goedemans, Senada Koljenović, Elisabeth Bloemena, Peter J. F. Snijders, Arko Gorter, and Sjoerd van der Burg.

References

1. Westra, W. H. The changing face of head and neck cancer in the 21st century: the impact of HPV on the epidemiology and pathology of oral cancer. *Head Neck Pathol.* **3** (1), 78-81 (2009).
2. Rietbergen, M. M. *et al.* Human papillomavirus detection and comorbidity: critical issues in selection of patients with oropharyngeal cancer for treatment De-escalation trials. *Ann Oncol.* **24** (11), 2740-2745 (2013).
3. Wallis, S. P., Stafford, N. D., Greenman, J. Clinical relevance of immune parameters in the tumor microenvironment of head and neck cancers. *Head Neck.* **37** (3), 449-459 (2015).
4. Ye, J., Livergood, R. S., Peng, G. The role and regulation of human Th17 cells in tumor immunity. *Am J Pathol.* **182** (1), 10-20 (2013).
5. Amedei, A. *et al.* Ex vivo analysis of pancreatic cancer-infiltrating T lymphocytes reveals that ENO-specific Tregs accumulate in tumor tissue and inhibit Th1/Th17 effector cell functions. *Cancer Immunol Immunother.* **62** (7), 1249-1260 (2013).
6. Whiteside, T. L. What are regulatory T cells (Treg) regulating in cancer and why? *Semin Cancer Biol.* **22** (4), 327-334 (2012).
7. Punt, S. *et al.* Angels and demons: Th17 cells represent a beneficial response, while neutrophil IL-17 is associated with poor prognosis in squamous cervical cancer. *Oncoimmunology.* **4** (1), e984539 (2015).
8. Bamias, A. *et al.* Significant differences of lymphocytes isolated from ascites of patients with ovarian cancer compared to blood and tumor lymphocytes. Association of CD3+CD56+ cells with platinum resistance. *Gynecol Oncol.* **106** (1), 75-81 (2007).
9. Gasparoto, T. H. *et al.* Patients with oral squamous cell carcinoma are characterized by increased frequency of suppressive regulatory T cells in the blood and tumor microenvironment. *Cancer Immunol Immunother.* **59** (6), 819-828 (2010).
10. Jordanova, E. S. *et al.* Human leukocyte antigen class I, MHC class I chain-related molecule A, and CD8+/regulatory T-cell ratio: which variable determines survival of cervical cancer patients? *Clin Cancer Res.* **14** (7), 2028-2035 (2008).
11. van Esch, E. M. *et al.* Alterations in classical and nonclassical HLA expression in recurrent and progressive HPV-induced usual vulvar intraepithelial neoplasia and implications for immunotherapy. *Int J Cancer.* **135** (4), 830-842 (2014).
12. Heeren, A. M. *et al.* Prognostic effect of different PD-L1 expression patterns in squamous cell carcinoma and adenocarcinoma of the cervix. *Mod Pathol.* **29** (7), 753-763 (2016).
13. Punt, S. *et al.* A beneficial tumor microenvironment in oropharyngeal squamous cell carcinoma is characterized by a high T cell and low IL-17(+) cell frequency. *Cancer Immunol Immunother.* **65** (4), 393-403 (2016).
14. Kirkwood, B. R., Sterne, J. A. C. *Essential Medical Statistics, 2nd edition.* Wiley-Blackwell. (2003).
15. Kleinbaum, D. G., Klein, M. *Survival Analysis: A Self-Learning Text, 2nd edition.* Springer. (2005).
16. Fabre, J. *et al.* Targeting the Tumor Microenvironment: The Protumor Effects of IL-17 Related to Cancer Type. *Int J Mol Sci.* **17** (9) (2016).
17. Feng, Z. *et al.* Multispectral imaging of formalin-fixed tissue predicts ability to generate tumor-infiltrating lymphocytes from melanoma. *J Immunother Cancer.* **3** (47) (2015).

Copyright © 2017 Journal of Visualized Experiments